Resilience Planning Model of Flexible Resources Collaborative under Typhoon Disaster

Xue Wu
School of Electrical Engineering
Beijing Jiaotong University
Beijing, China
23121492@bjtu.edu.cn

Dahai Zhang*
School of Electrical Engineering
Beijing Jiaotong University
Beijing, China
dhzhang1@bjtu.edu.cn
*Corresponding author

Xinxin Zheng
School of Electrical Engineering
Beijing Jiaotong University
Beijing, China
22110446@bjtu.edu.cn

2024 IEEE International Conference on Energy Internet (ICEI) | 979-8-3315-2355-8/24/$31.00 ©2024 IEEE | DOI: 10.1109/ICEI63732.2024.10917096

***Abstract*—Aiming at the problems brought by typhoon disaster to the safe operation of power system, this paper puts forward a cooperative resilience planning model of multiple flexible resources under typhoon disaster. Firstly, the failure rate of each branch is obtained according to the typhoon disaster disturbance and line failure rate model, and the information entropy method is used to identify the vulnerable lines. Then, flexible resources such as wind power, photovoltaic energy storage and line reinforcement are used to coordinate planning to improve system resilience. A two-stage three-layer defense-attack-defense model is constructed considering system economy and resilience, and the Column and Constraint Generation (C&CG) algorithm is used to solve the model. Finally, the effectiveness of the proposed model is verified by the IEEE30-node system.**

Keywords—Typhoon disaster, Resilience planning, Flexible resources, Collaborative planning

I. INTRODUCTION

The power system is vulnerable to extreme natural disasters, which brings great risks to the safe and reliable operation of the power system [1]. For example, in 2019, super Typhoon Lekima caused a total of 168 power outages of 110kV and above lines in several provinces [2]. In order to reduce the impact of extreme disasters, it is urgent to carry out resilience planning for power system to improve the resilience level of the system and reduce the load loss under extreme disasters.

In this paper, the typhoon disaster scenario is used for analysis. The typhoon disaster has spatio-temporal characteristics, which makes the failure time and location have strong uncertainty. To deal with uncertainty, the current research mainly adopts random programming [3] and robust programming [4]. Random programming assumes that random variables follow a certain probability distribution, but due to the low probability of extreme disasters, there is a deviation between the probability distribution fitted with historical data and the real distribution. Therefore, this paper considers adopting robust planning method, which generally adopts N-K criterion to establish fault uncertainty set. Then, the resilience of the power system is studied under the worst fault scenario in the fault uncertainty set [5]. Reference [6] used typhoon Batts model to generate wind speed curves of lines, and combined the vulnerability model of poles and wires to create distribution network fault scenarios through Monte Carlo simulation. However, Monte Carlo simulation method requires a lot of computing resources and time to ensure the accuracy of the results, and the calculation speed is slow when the number of components is large. Therefore, after the failure rate of each component is obtained, how to describe the fault state of each component quickly and efficiently is an urgent problem to be solved.

The flexible resources in the source network load have great potential for the resilience improvement of the new power system. Exploiting the resilient potential of the system flexible resources has guiding significance for the resilience planning and decision-making of the power system. Reference [7] studied the influence of typhoon disaster on rod fall and line break, and adopted two-layer planning method of fixed capacity siting with flexible resources such as gas turbines, energy storage and electric vehicles to enhance the resilience of distribution network. Reference [8] proposed a method to improve the resilience of distribution network through line reinforcement, SOP, energy storage and coordinated scheduling of generators. Reference [9] proposed a two-tier distribution network planning method that considers the flexible resource coordination of source, load and storage at the same time, so as to achieve higher economy. However, at present, cooperative planning of flexible resources mostly occurs in the distribution network. For the power system, the potential of flexibility resources in all aspects of source network load has not been fully tapped, which needs further research.

In view of the above problems, this paper proposes a flexible resource collaborative resilience planning model for typhoon disasters. The main contributions include: 1) In view of the uncertainty of typhoon disaster, the information entropy method is used to describe the uncertainty of the fault state of the line on the basis of obtaining the fault rate of the line; 2) The collaborative planning of multiple flexible resources is used to improve the resilience of the system. Before the disaster, the configuration of energy storage, wind power and photovoltaic and line reinforcement are used to improve the resilience of the system. After the disaster, the maintenance of maintenance teams and dynamic scheduling of generator sets, energy storage,

Supported by National Natural Science Foundation of Smart Grid Joint Fund: Theory and method of new power system intelligent planning for resilient enhancement (U22B20103).

wind power and photovoltaic are considered to achieve rapid load recovery.

II. Research Framework of Resilience Planning Model

A. Model of Spatio-temporal Evolution of Typhoons

1) Typhoon disaster disturbance model

In order to accurately simulate typhoon wind speed and wind direction change, typhoon wind field models such as Batts, Shapiro and YanMeng models are used in the project [10]. The Batts model is used in this paper. The wind speed in the area around the typhoon is related to the distance r from the typhoon center:

$$V_r = \begin{cases} \dfrac{V_{R_{\max}} r}{R_{\max}}, r \le R_{\max} \\ V_{R_{\max}} (\dfrac{R_{\max}}{r})^x, r > R_{\max} \end{cases} \quad (1)$$

where: $V_{R_{\max}}$ represents the maximum wind speed of the typhoon, which is 39.54m/s in this paper; $R_{\max}$ is the maximum wind radius of the typhoon, which is 45km in this paper. x is the intensity attenuation coefficient, which is taken as 0.6 in this paper.

2) Line failure rate model

When all the wires and poles between the two nodes are in normal operation, the corresponding branch can operate normally. Therefore, the branch failure rate model needs to consider connecting the wires and poles in series:

$$p_{ij}(s) = 1 - (1 - p_l(s))^{m_{ij}} (1 - p_p(s))^{y_{ij}} \quad (2)$$

where: $p_{ij}(s)$ is the failure rate of branch ij when the typhoon intensity is s, $p_l(s)$ and $p_p(s)$ are the failure rates of conductors and poles, respectively, m_{ij} and y_{ij} are the number of wires and poles corresponding to the branch.

B. Research Framework of Resilience Planning Model

This paper constructs a two-stage resilience planning model research framework for pre-disaster defense and post-disaster recovery, as shown in Fig. 1.

On the basis of obtaining the line failure rate, a two-stage robust resilient planning model is established based on the defense-attack-defense (DAD) structure. The first stage is the first layer of the DAD model, which is the pre-disaster defense stage. Its planning objective is to minimize the line reinforcement cost and the on-duty installation cost of flexible resources such as energy storage, wind power, and photovoltaic, and the decision variables are transferred to the second stage. The second stage includes the second layer and the third layer of the DAD model. The second layer, in the disaster occurrence stage, determines the worst failure scenario and transmits the worst failure scenario to the third layer. The objective of the third layer planning is to minimize the loss load cost and system operation cost, while achieving power system fault recovery by considering the maintenance team's participation in repairs and the dynamic scheduling of flexible resources. The worst fault scenario and recovery strategy obtained in the second stage are fed back to the first stage to adjust the planning decision. Finally, the most reasonable planning decision scheme is obtained through iteration.

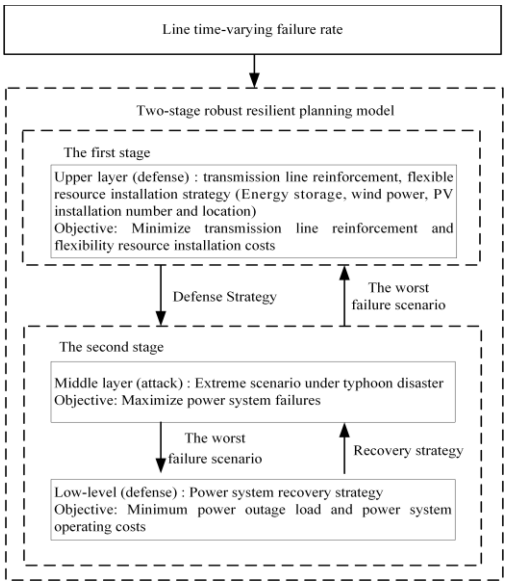

Fig. 1. Research framework of resilience planning model

III. Resilience Planning Model of Power System

A. Objective Function

The objective function considered by the model is line reinforcement cost and on-duty installation cost of energy storage, wind power, photovoltaic and other flexible resources in the first stage, as well as lost load and system operation cost in the second stage. The expression of the objective function is as follows:

$$\min_{\substack{x_l, \alpha_i^{ESS}, \alpha_i^{pw}, \alpha_i^{pv}, \\ K_E, K_w, K_p}} \sum_{l \in \Omega_L} C_{L,l} x_l + C_p + \max_{u \in U} \min_{\substack{\Delta P_i^D, P_{ij}, P_i^G, \\ P_i^{pw}, P_i^{pv}, P_i^{ESS}}} \sum_{i \in \Omega_N} C_{D,i} \Delta P_i^D + C_o \quad (3)$$

$$C_p = \sum_{i \in \Omega_N} \frac{r(1+r)^s}{r(1+r)^s - 1} (C_{ESS} \alpha_i^{ESS} K_E + C_{pw} \alpha_i^{pw} K_w + C_{pv} \alpha_i^{pv} K_p) / Y \quad (4)$$

$$C_o = \sum_{i \in \Omega_G} C_{G,i} P_i^G + \sum_{i \in \Omega_N} (C_{e,op} P_i^{ESS} + C_{w,op} P_i^{pw} + C_{p,op} P_i^{pv}) \quad (5)$$

where, $\Omega_L, \Omega_G, \Omega_N$ respectively represent the collection of transmission lines, generator sets and load nodes; $C_{L,l}$ is the reinforcement cost of the l transmission line. x_l represents the 0/1 decision variable, indicating the state of the line reinforcement. If the value is 1, it is reinforced. Otherwise, it is not reinforced. α_i^{ESS}、α_i^{pw} and α_i^{pv} are all 0/1 variables, indicating whether energy storage, wind power and PV are connected to the node respectively. If their values are 1, they are connected to node i; if they are 0, they are not connected to node i. $C_{L,l}$ is the reinforcement cost of the line in the first stage; C_p is the on-duty installation cost of energy storage, wind power and photovoltaic; C_{ESS}、C_{pw} and C_{pv} respectively represent the installation cost of energy storage, wind power

and photovoltaic; K_E、K_w and K_p respectively represent the installed capacity of energy storage, wind power and photovoltaic. *r* is the discount rate, *s* is the number of discount times, and *Y* is the total number of days in a year. *u*/*U* represents a certain fault state/fault state set of the power system under the typhoon disaster in the middle layer; P_{ij} is the active power of the branch, P_i^G is the active power output of the generator set *i*, P_i^{pw}、P_i^{pv}、P_i^{ESS} are the active power output of installed wind power, photovoltaic and energy storage respectively. $C_{D,i}$ is the load cutting penalty cost of node *i*. In this paper, according to the importance of load, loads are divided into important load and conventional load, and the weight ratio of penalty cost of important load and conventional load is set as 10, and ΔP_i^D is the load loss amount of node *i*. C_o represents the operating cost of the system, $C_{G,i}$ represents the operating cost of the generator set *i*, $C_{e,op}$、$C_{w,op}$、$C_{p,op}$ are the operating cost coefficients of energy storage, wind power and photovoltaic.

B. First-stage Constraint

Through the pre-disaster line reinforcement, the optimal configuration of ESS, wind power and photovoltaic to enhance the resilience of the power system. The constraints of the upper-layer defense model are as follows:

$$\sum_{l\in\Omega_L} x_l \le N_L \tag{6}$$

$$\sum_{i\in\Omega_N} \alpha_i^{ESS} \le N_{ESS} \tag{7}$$

$$\sum_{i\in\Omega_N} \alpha_i^{pw} \le N_{pw} \tag{8}$$

$$\sum_{i\in\Omega_N} \alpha_i^{pv} \le N_{pv} \tag{9}$$

$$0 \le P_i^{ESS} \le \alpha_i^{ESS} P_{ESS}^{\max}, \forall i \in \Omega_N \tag{10}$$

$$0 \le P_i^{pw} \le \alpha_i^{pw} \delta_{pw} K_w, \ \forall i \in \Omega_N \tag{11}$$

$$0 \le P_i^{pv} \le \alpha_i^{pv} \delta_{pv} K_p, \ \forall i \in \Omega_N \tag{12}$$

Where, N_L, N_{ESS}, N_{pw} and N_{pv} represent the maximum number of line reinforcement and the maximum number of installed energy storage, wind power and photovoltaic respectively. $P_{ESS}^{\max}$ represents the maximum discharge power of energy storage. δ_{pw} and δ_{pv} represent the normalized wind power and photovoltaic power output series, respectively, which are based on 8760h data of a regional power grid.

C. Second-stage Constraint

1) Uncertainty of failure state of power system

In this paper, information entropy is used to describe the uncertainty of fault state, which is mainly determined based on the failure rate of each line under typhoon disaster and the fault repair time of the system. The fault state uncertainty model constructed is as follows:

$$U = \left\{ u \left| \sum_{ij\in\Omega_L} (-\log_2 p_{ij,t})(1-z_{ij,t}) \le \Gamma \right. \right. \tag{13}$$

$$\sum_{t\in T} (1-z_{ij,t}) \le 1 \tag{14}$$

$$1-u_{ij,t} = \sum_{\gamma=\max\{1,t-T_{s,ij}\}}^{t} (1-z_{ij,\gamma}), \forall ij \in \Omega_L, \forall \gamma, t \in T \tag{15}$$

Where, $p_{ij,t}$ represents the failure rate of line *ij* at time *t*, $z_{ij,t}$ and $u_{ij,t}$ are both 0-1 decision variables, $z_{ij,t}$ represents the fault state of line *ij* under typhoon attack at time *t*, and its value 0 indicates that the line fails after typhoon attack, and vice versa is 1. However, $u_{ij,t}$ represents the actual fault state of line *ij* at time *t* after the typhoon attack, and its value is 0, indicating that the line is in fault state; otherwise, the value is 1. Γ represents the budget value of information entropy, $T_{s,ij}$ is the time to repair the faulty line *ij*.

2) Line state constraint

$$\alpha_{ij,t} = 1-(1-u_{ij,t})(1-x_l), \forall ij, l \in \Omega_L, \forall t \in T \tag{16}$$

Where, $\alpha_{ij,t}$ is the 0-1 decision variable, which represents the running state of the line under typhoon attack after reinforcement. If the line is in normal running state, its value is 1; otherwise, it is 0. Formula (16) indicates that the line strengthened in the first stage will not fail due to typhoon attack.

3) Power balance constraint

$$\sum_{i\in\Omega_N} (P_i^D - \triangle P_i^D) = \sum_{i\in\Omega_G} P_i^G + \sum_{i\in\Omega_N} (P_i^{pw} + P_i^{pv} + P_i^{ESS}) + \sum_{ij\in\Omega_n^+} P_{ij,t} - \sum_{ij\in\Omega_n^-} P_{ij,t} \tag{17}$$

Where, Ω_n^+、Ω_n^- are the line sets of the outgoing and incoming power of node *n*, $P_{ij,t}$ is the power of branch *ij* at time *t*, and P_i^D is the load of each node.

4) Load reduction constraint

$$0 \le \Delta P_i^D \le P_{i,\max}^D \tag{18}$$

where: $P_{i,\max}^D$ is the maximum load of each node.

5) Energy storage operation constraint

Considering the scarcity of power supply resources after disaster, this paper only considers the discharge behavior of energy storage in the fault recovery stage.

$$0 \le P_{i,t}^{ESS} \le P_i^{ESS}, \forall i \in \Omega_N, \forall t \in T \tag{19}$$

$$E_{i,t}^{ESS} = E_{i,t-1}^{ESS} - \frac{P_{i,t-1}^{ESS}}{\eta^E} \times \Delta t, \forall i \in \Omega_N, t > 1 \tag{20}$$

$$E_{i,t}^{ESS} = 0.6 K_E, \forall i \in \Omega_N, t = 1 \tag{21}$$

$$\underline{S}_{oc} K_E \le E_{i,t}^{ESS} \le \overline{S}_{oc} K_E, \forall i \in \Omega_N, \forall t \in T \tag{22}$$

where, $E_{i,t}^{ESS}$ represents the charge of the stored energy at time t, η^E represents the discharge efficiency of the stored energy, $\overline{S}_{oc}$、$\underline{S}_{oc}$ are the upper and lower limits of the state of charge of the stored energy, respectively.

IV. Solution of Model

In this paper, C&CG algorithm is used to solve the two-stage robust resilient enhancement model constructed above. First, the original problem is transformed into the following compact form:

$$\min_x \{c^T x + \max_{u\in U} \min_{y\in\Omega(x,u)} d^T y\} \tag{23}$$

$$s.t \quad Ax \le b \tag{24}$$

$$\begin{aligned} &\Omega(x,u) = \{Dy \le f \\ &Ey = g,\ Fy = u \\ &Gx + Hu + Iy \le h\} \end{aligned} \tag{25}$$

where: x is the set of decision variables in the first stage, and y is the set of decision variables in the second stage; A、D、E、F、G、H、I are the coefficient matrixs, c、d、b、f、g、h are constant vectors, $\Omega(x,u)$ is the feasible domain of decision variable y in the second stage. Equation (24) contains constraint expressions (6) to (12), and equation (25) contains expressions (13) to (22) of the second stage. The original problem is decomposed into main problem and subproblem to achieve alternating iterative solution.

A. Main Problem

Based on the C&CG algorithm, the expression of the main problem is:

$$\begin{aligned} &\min_x c^T x + \eta \\ &s.t.\ \ Ax \le b \\ &\quad \eta \ge d^T y_l \\ &\quad Dy_l \le f \\ &\quad Ey_l = g \\ &\quad Gx + Iy_l \le h - Hu_l \end{aligned} \tag{26}$$

where, y_l is the solution of the subproblem obtained by the l iteration; u_l is the value obtained in the l iteration in the worst scenario, that is, the most serious line fault state; η is the cut plane value.

B. Subproblem

Based on the defense strategy determined by the main problem, the sub-problem will determine the "worst" scenario and update the recovery strategy by adopting the corresponding scheduling scheme. The mathematical model of the sub-problem can be expressed as:

$$\max_{u\in U} \min_{y\in\Omega(x,u)} d^T y \tag{27}$$

$$\begin{aligned} &s.t.\ \ Dy \le f : \alpha \\ &\quad Ey = g : \beta \\ &\quad Fy = u : \gamma \\ &\quad Iy \le h - Gx - Hu : \varphi \end{aligned} \tag{28}$$

The constraints of the subproblem include all the constraints of the second stage. Since the subproblem is a two-layer optimization problem, it is necessary to use the strong duality theory to find the dual problem of the inner layer minimization problem, and transform the two-layer problem into a single-layer problem for solving. In addition, the dual variables corresponding to each constraint of equation (28) are respectively α、β、γ、φ. The specific form of the single-layer max problem transformed after the dual transformation is as follows:

$$\begin{aligned} &\phi = \max_{u\in U} \max_{\alpha、\beta、\gamma、\varphi} \alpha^T f + \beta^T g + \gamma^T u + (h - Gx - Hu)^T \varphi \\ &s.t. \qquad D^T\alpha + E^T\beta + F^T\gamma + I^T\varphi \le d \\ &\qquad \alpha \le 0 \quad \varphi \le 0 \end{aligned} \tag{29}$$

C. Solution Step

Firstly, the master problem is solved to obtain the optimal solution and the lower bound value L_B is updated. Then, according to the line reinforcement and flexible resource allocation strategy solved by the main problem, the dual transform sub-problem is solved to determine the most serious line fault state and the corresponding recovery strategy to update the upper bound value U_B; Finally, determine whether $|U_B - L_B| / U_B \le \varsigma$ is satisfied, where ς is the convergence threshold, if not, the solved worst-case scenario is passed to the main problem to adjust the update prevention strategy.

V. Example Analysis

In order to verify the performance of the model constructed in this paper, simulation analysis is carried out on the IEEE30-node system, which contains 6 generators, 41 transmission lines, the total load of the system is 5300MW, and the total installed capacity is 5400MW. The system topology diagram is shown in Fig. 2. The price parameters of the system and the configuration parameters of the energy storage/wind power/photovoltaic device are shown in Table I.

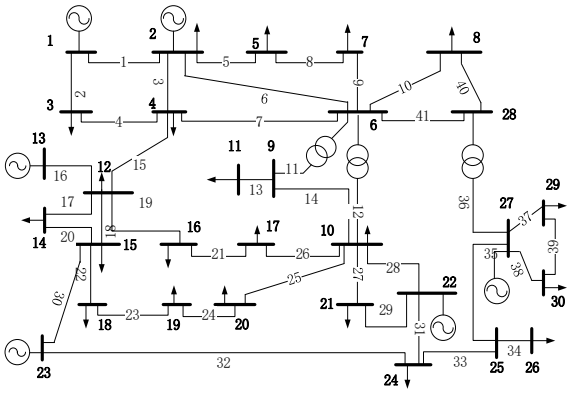

Fig. 2. The IEEE 30-bus system topology diagram

TABLE I. SYSTEM PRICE PARAMETERS AND STORAGE/WIND/PV DEPLOYMENT PARAMETERS

System price parameters	Value	ESS/wind/PV deployment parameters	Value
$C_{L,l}$	800000(yuan/km)	K_E	800(MW)
C_{ESS}	1800000(yuan/MW)	K_w	500(MW)
C_{pw}	2000000(yuan/MW)	K_p	300(MW)
C_{pv}	1200000(yuan/MW)	$P_{ESS}^{\max}$	300(MW)
$C_{D,i}$	1000/10000(yuan/MW)	η^E	0.8
$C_{e,op}$	52(yuan/MW)	$\underline{S}_{oc}$ / $\overline{S}_{oc}$	0.1/0.9
$C_{w,op}$ / $C_{p,op}$	170/150(yuan/MW)	r / s	0.06/10

A. *Typhoon Disaster Scenario Simulation*

Assume that the eye coordinates of the typhoon at the beginning of the typhoon are (-20, -20)km, the typhoon moves at the speed of 20km/h, and the angle between the path and the horizontal coordinate is 45°. According to the typhoon disaster disturbance model, the moving path of the typhoon after landing can be obtained, as shown in Fig. 3, where the red dashed circle indicates the range of the typhoon wind field at each time period. Based on the line failure rate model, the branch failure rate curve shown in Fig. 4 is obtained.

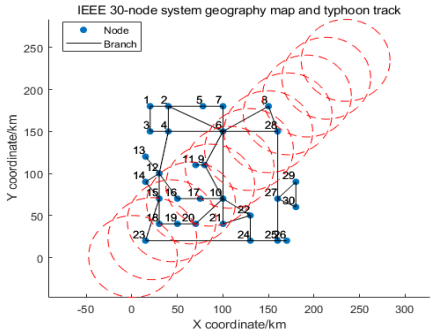

Fig. 3. IEEE 30-node system geography map and typhoon track

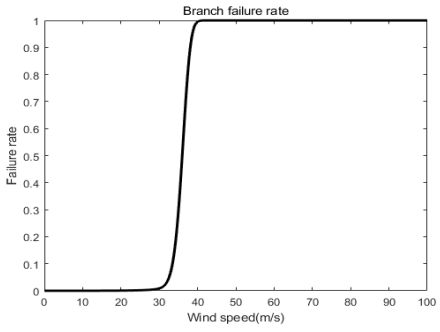

Fig. 4. Branch failure rate curve

As can be seen from Fig. 4, when the wind speed exceeds 30m/s, the failure rate of the branch increases significantly. As the typhoon moves, the wind speed on the branch increases gradually and reaches its maximum at the radius of the maximum wind speed. However, when the branch is inside or outside the typhoon wind field, the wind speed on the branch decreases on the contrary, so the time-varying failure rate curve of the branch in Fig. 5 will show two peaks.

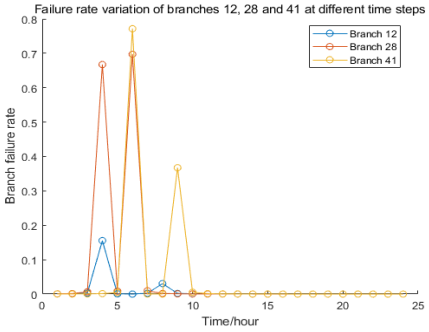

Fig. 5. 12/28/41 branch time-varying failure rate

B. *Performance Analysis of Resilient Planning Schemes*

In order to test the performance of different planning schemes for the improvement of system resilience, this paper sets up four schemes for comparative analysis. Scheme 1: No planning measures are considered; Scheme 2: Only consider the configuration of wind power photovoltaic; Scheme 3: Consider the configuration of wind power PV and energy storage; Scheme 4: Comprehensively consider the configuration of wind power, photovoltaic, energy storage and line reinforcement measures. In this section, the number of line reinforcement is set to 3; the number of wind power, photovoltaic, and energy storage configurations is set to 2, 2, and 3 respectively; the budget value of information entropy is set to 1.6, and the convergence threshold of C&CG algorithm is set to 1.0e-3.

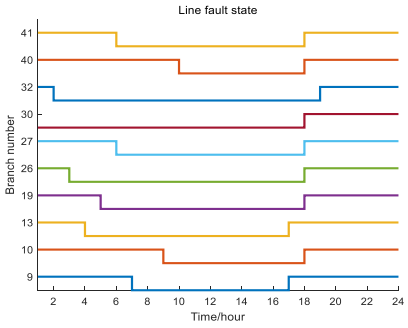

Fig. 6. Scheme 1 line fault status

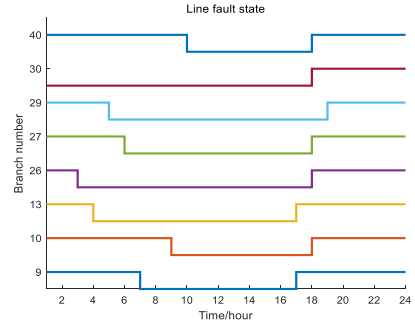

Fig. 7. Scheme 4 line fault status

Fig. 6 shows the fault state of the line in scheme 1, and the dented part in the figure indicates that the line is in the fault state. Scheme 1 is severely damaged by typhoon because planning measures are not considered, and the number of faulty lines is as high as 10.

Fig. 7 shows the line fault state in the worst scenario obtained by scheme 4. Since the line reinforcement measures are taken into account, the number of fault branches is reduced compared with scheme 1. In this paper, it is assumed that the typhoon disaster starts at t = 1 and ends at t = 13, after which the maintenance team starts maintenance. Assuming that the geographical location of the maintenance department is located at node 1 (20,180) and the maintenance resources are sufficient, that is, each faulty branch can be repaired in the first time, and the normal average traveling speed of the maintenance team is 60km/h. The average repair time of each line is 3h. The repair time of each faulty line is shown in Table II.

TABLE II. FAULTY BRANCH AND RECOVERY TIME

Fault branch	Start time of failure (h)	Repair time (h)	End time of failure (h)
9	7	4	17
10	9	5	18
13	4	4	17
26	3	5	18
27	6	5	18
29	5	6	19
30	1	5	18
40	10	5	18

As can be seen from Table II, the branch that is first affected by the typhoon, such as Branch 30, has the earliest failure. As the typhoon moves, the final affected areas, such as branch roads 10 and 40, also begin to fail. Therefore, typhoons with temporal and spatial characteristics cause different positions and different numbers of line faults in different periods, which indicates that the temporal and spatial evolution model of typhoons can effectively simulate the uncertainty of power system faults caused by the time-varying characteristics of typhoons.

Scheme 1 and Scheme 4 are taken as examples to analyze the planning scheme. The topology of the planning result of Scheme 1 and Scheme 4 is shown in Fig. 8 and Fig. 9 respectively. As can be seen from Fig. 8, the failure of branch 13 leads to the loss of power supply for critical load 11, the failure of branch 19 and 26 leads to the loss of power supply for critical load 17, and the failure of branch 30 and 32 leads to the failure of thermal power units at node 23 to transmit power to the system. The power loss of critical loads will cause great impact, and effective measures should be taken to ensure the power supply of important loads.

Compared with scheme 1, scheme 4 can ensure the power supply of all critical loads and reduce the power loss load of the system. The deployment results of scheme 4 planning measures are shown in Fig. 9. Lines 19, 32 and 41 are reinforced, so that they will not fail under typhoon disasters, so that the thermal power units at node 23 can effectively transmit electric energy to the system and ensure the power supply of important load 17. Nodes 9 and 12 are equipped with wind turbines, nodes 11 and 16 are equipped with photovoltaic, and nodes 4, 8 and 14 are installed with energy storage devices. The configuration of these flexible resources can not only prioritize the power supply of critical loads, but also reduce the power loss of conventional loads. Therefore, the cooperative planning of multiple flexible resources can effectively reduce the power loss load and improve the resilience of the system.

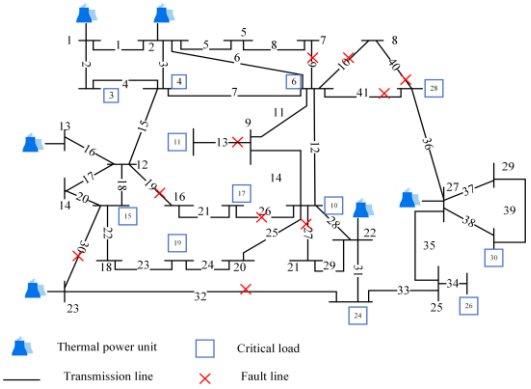

Fig. 8. Planning results of Scheme 1

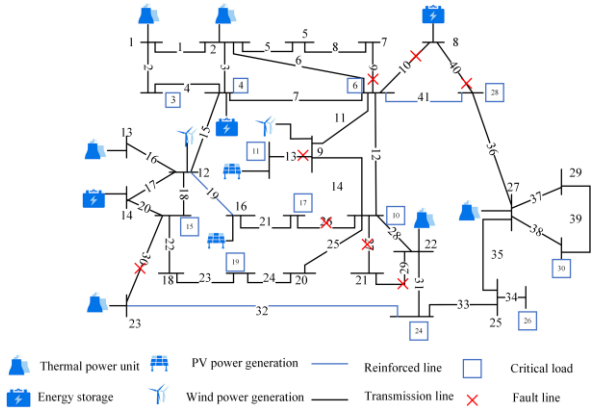

Fig. 9. Planning results of Scheme 4

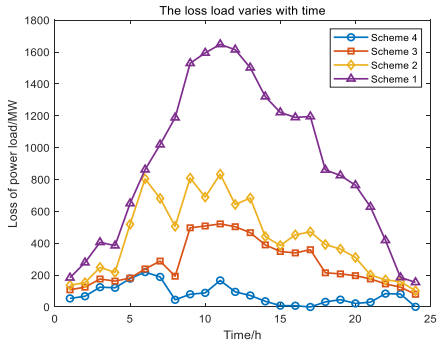

Fig. 10. The loss load varies with time

The changes of power loss load of the above four planning schemes are shown in Fig. 10. It can be seen that scheme 1, which does not take any planning measures, has the largest power loss load, while scheme 4, which comprehensively considers the configuration of wind power, photovoltaic power storage and line reinforcement measures, has the least power loss load. Therefore, cooperative planning of multiple flexible resources can effectively reduce the system's power loss load

and improve the system resilience. It can be seen from the figure that after the typhoon ends at time t = 13, the load loss of the four planning schemes gradually decreases due to the maintenance team participating in the maintenance.

The planning cost, operation cost and lost load cost of the above four planning schemes can be obtained through simulation experiments, as shown in Table III. It can be seen from Table III that compared with scheme 1, which does not take any planning measures, the loss load of schemes 2-4 gradually decreases, so the lost load cost gradually decreases, which further indicates that cooperative planning of multiple flexible resources can effectively improve the resilience of the system.

The access of wind power and photovoltaic in scheme 2 reduces the load loss of the system, but the output of wind power and photovoltaic leads to additional operating expenses, and the generator output at this time has no great change compared with scheme 1, so the operating cost is slightly increased compared with scheme 1. For scheme 3, due to the configuration of energy storage device, the output of the generator set is reduced, and the operating cost of wind power, photovoltaic and energy storage is less than that of the generator set, so the operating cost is reduced. The reinforcement of the line in scheme 4 reduces the load loss of the system, increases the output of wind power, photovoltaic and energy storage, and further reduces the output of the generator set, so the operating cost is further reduced. Compared with scheme 1, which does not take any planning measures, the total cost of scheme 2-4 is gradually reduced, indicating that the coordinated planning of multiple flexible resources can not only effectively improve the resilience of the power system, but also reduce the economic losses caused by typhoons.

TABLE III. COST OF RESILIENCE PLANNING MEASURES UNDER DIFFERENT SCHEMES(TEN THOUSAND YUAN)

Scheme	1	2	3	4
Wind power installation cost	\	74.45	74.45	74.45
Photovoltaic Installation cost	\	26.8	26.8	26.8
Energy storage Installation Cost	\	\	150.76	150.76
Line reinforcement cost	\	\	\	240
Lost load cost	8799.0	2302.3	1032.2	195.5
Operation cost	2778.0	2938.8	2365.9	2264.6
Total cost	11577.0	5342.4	3651.1	2952.1

VI. CONCLUSION

Aiming at the uncertainty of power system fault state under typhoon disaster, this paper comprehensively considers the economy and resilience of the system, and proposes a two-stage robust resilient programming model for cooperative planning of multiple flexible resources, which is solved by C&CG algorithm. Finally, the validity of the constructed model is verified by a numerical example, and the conclusions are as follows:

(1) According to the time-varying failure rate of the line, the information entropy is used to identify the vulnerable line, and the time-varying fault state of each line can be obtained.

(2) Through the analysis of the performance of the resilient planning scheme, it is concluded that the coordinated planning of multiple flexible resources can not only effectively improve the resilience of the power system, but also reduce the economic losses caused by typhoon disasters.

ACKNOWLEDGMENT

This work is supported by National Natural Science Foundation of Smart Grid Joint Fund: Theory and method of new power system intelligent planning for resilient enhancement (U22B20103).

REFERENCES

[1] Bei Chaohong, Lin Chaofan, Li Gengfeng, et al. Development and prospect of flexible power system under Energy transition [J]. Proceedings of the CSEE, 2020, 40(9): 2735-2745.

[2] Zhang Yi. Impact of super Typhoon on Zhejiang power grid and prevention suggestions [J]. Journal of Zhejiang Institute of Water Resources and Hydropower, 2020, 32(4): 39-44.

[3] Ma S, Li S, Wang Z, et al. Resilience-Oriented Design of Distribution Systems[J]. IEEE Transactions on Power Systems, Institute of Electrical and Electronics Engineers Inc., 2019, 34(4): 2880–2891.

[4] Lin Y, Bie Z. Tri-level optimal hardening plan for a resilient distribution system considering reconfiguration and DG islanding[J]. Applied Energy, Elsevier Ltd, 2018, 210: 1266–1279.

[5] Wang X, Li Z, Shahidehpour M, et al. Robust Line Hardening Strategies for Improving the Resilience of Distribution Systems with Variable Renewable Resources[J]. IEEE Transactions on Sustainable Energy, Institute of Electrical and Electronics Engineers Inc., 2019, 10(1): 386–395.

[6] Du Yaxin. Distribution Network elastic modeling and evaluation method considering multi-energy coupling [D]. Shandong University, 2020.

[7] Ma Liye, Wang Haifeng, Lu Zhigang, et al. Enhanced Distribution Network Resilience and flexibility resource planning under Typhoon disaster with Correlation Effect [J]. Automation of Electric power Systems, 2022, 46(7): 60-68.

[8] Huang Z, Zhang Y, Xie S. A comprehensive strategy for the distribution network resilience enhancement considering the time-varying behaviors of typhoon path[J]. Electric Power Systems Research, Elsevier Ltd, 2023, 214.

[9] Gao Hui, Yan Hanting, Huang Chunyan. Two-layer planning of active distribution network considering "source-load-storage" flexible resource coordination [J]. Guangdong Electric Power, 2019, 32(5): 29-35.

[10] Lin Peiyuan, Wen Zeguo, Liu Haipeng, et al. YanMeng wind field model for calculating extreme wind speed in Guangdong engineering sea area [J]. Journal of Natural Disasters, 2022, 31(6): 104-112.